ACL Fibers Near the Lateral Intercondylar Ridge Are the Most Load Bearing During Stability Examinations and Isometric Through Passive Flexion

Danyal H. Nawabi,*‡ MD, FRCS, Scott Tucker,† MEng, Kevin A. Schafer,† BS,
Hendrik Aernout Zuiderbaan,‡ MD, PhD, Joseph T. Nguyen, Thomas L. Wickiewicz,‡ MD,
Carl W. Imhauser,† PhD, and Andrew D. Pearle,‡ MD
*Investigation performed at the Department of Biomechanics, Hospital for Special Surgery,
New York, New York, USA*

Background: The femoral insertion of the anterior cruciate ligament (ACL) has direct and indirect fiber types located within the respective high (anterior) and low (posterior) regions of the femoral footprint.

Hypothesis: The fibers in the high region of the ACL footprint carry more force and are more isometric than the fibers in the low region of the ACL footprint.

Study Design: Controlled laboratory study.

Methods: Ten fresh-frozen cadaveric knees were mounted to a robotic manipulator. A 134-N anterior force at 30° and 90° of flexion and combined valgus (8 N·m) and internal (4 N·m) rotation torques at 15° of flexion were applied simulating tests of anterior and rotatory stability. The ACL was sectioned at the femoral footprint by detaching either the higher band of fibers neighboring the lateral intercondylar ridge in the region of the direct insertion or the posterior, crescent-shaped fibers in the region of the indirect insertion, followed by the remainder of the ACL. The kinematics of the ACL-intact knee was replayed, and the reduction in force due to each sectioned portion of insertion fibers was measured. Isometry was assessed at anteromedial, center, and posterolateral locations within the high and low regions of the femoral footprint.

Results: With an anterior tibial force at 30° of flexion, the high fibers carried 83.9% of the total anterior ACL load compared with 16.1% in the low fibers (*P* < .001). The high fibers also carried more anterior force than the low fibers at 90° of flexion (95.2% vs 4.8%; *P* < .001). Under combined torques at 15° of flexion, the high fibers carried 84.2% of the anterior ACL force compared with 15.8% in the low fibers (*P* < .001). Virtual ACL fibers placed at the anteromedial portion of the high region of the femoral footprint were the most isometric, with a maximum length change of 3.9 ± 1.5 mm.

Conclusion: ACL fibers located high within the femoral footprint bear more force during stability testing and are more isometric during flexion than low fibers.

Clinical Relevance: It may be advantageous to create a ''higher'' femoral tunnel during ACL reconstruction at the lateral intercondylar ridge.

Keywords: ACL; direct insertion; indirect insertion; femoral footprint; force; isometry; lateral intercondylar ridge

The macroscopic anatomy of the femoral attachment of the anterior cruciate ligament (ACL) has been studied extensively, including reports of the shape and size of its insertional footprint.[8,13,26,33,38] However, the collagen fiber architecture comprising the ACL attachments has received less attention despite its critical role in transmitting load from the ACL substance to bone.[16,31] Previous histological observations of the femoral insertion by Iwahashi et al[16] identified distinct direct and indirect insertional anatomy.

The direct insertion is located anteriorly or higher on the medial aspect of the lateral femoral condyle and is connected to a bony depression parallel to and immediately posterior to the lateral intercondylar ridge.[8,9] The fiber architecture of the direct insertion suggests that it is an important load-bearing structure consisting of a band of dense collagen fibers with a zonal architecture transitioning from ligament to fibrocartilage to mineralized fibrocartilage and then to bone.[36] These direct fibers exist in a band extending 5.3 ± 1.1 mm posteriorly on average or slightly

more than half of the distance from the lateral intercondylar ridge to the posterior femoral articular cartilage.[31]

The indirect insertion appeared as a fan-like posterior extension of the ACL in full knee extension that reached the margin of the articular cartilage of the lateral femoral condyle and remained adherent to and lower on the wall of the intercondylar notch during flexion.[23] Histologically, the indirect insertion consisted of Sharpey fibers that extended posteriorly to blend into the articular cartilage of the posterior aspect of the lateral femoral condyle.[23] This tissue was located between the direct insertion and the posterior femoral articular cartilage and had an average width of 4.4 ± 0.5 mm in the anteroposterior direction.[31]

The stabilizing role of the direct and indirect portions of the femoral attachment of the ACL was reported by Pathare et al.[27] Specifically, arthroscopic debridement of the posterior aspect of the femoral footprint, which included fibers in the region of the indirect insertion, yielded minimal increases in anterior translation in response to uniplanar anterior loads and multiplanar rotatory loads simulating a pivot shift.[27] Thus, the direct insertion played a dominant role in resisting anterior translations. Yet how load was distributed across these 2 aspects of the femoral insertion was not explored.

Sectioning the ACL fibers located closer to the lateral intercondylar ridge at the central proximal region of the femoral attachment caused the largest drop in load (66%-84%) in response to anterior displacement of the tibia.[18] These central proximal fibers within the femoral footprint also resisted about 10% of the internal rotation torque generated when internally rotating the tibia by 10°. However, this study did not assess regional load transfer across the femoral insertion in response to multiplanar valgus and internal rotation torques, which impart greater loads in the ACL than internal rotation alone[17] and form an important subset of the loads applied during the pivot shift.[7,19,25,27] Moreover, the same tissue sectioning order was used across specimens; this fails to account for load sharing (ie, physical interaction) across the ligament midsubstance as described previously.[11,30]

Anatomic grafts placed in a less isometric location may increase graft loads. In fact, registry data indicate that anteromedial (AM) portal drilling, which may be associated with "lower" placement of femoral tunnels,[5] has led to increased rates of graft failure.[28] Therefore, quantifying load transfer patterns across the femoral footprint in combination with measurements of graft isometry might help guide graft placement during ACL reconstruction.

The purpose of this study was to (1) quantify the load transferred across the higher and lower portions of the femoral ACL footprint in the respective regions of the direct and indirect insertion fibers during stability testing and (2) determine the changes in length of virtual ACL fibers placed at different tunnel locations within the direct and indirect femoral insertions during passive flexion. It was hypothesized that the fibers in the high (more anterior) region of the ACL footprint carry more force and are more isometric than the fibers in the low (more posterior) region of the ACL footprint.

METHODS

Ten fresh-frozen human cadaveric knees were used in this study. The mean age of the specimens was 52.5 years (range, 29-65 years). Any specimen with evidence of bony deformity, ligament damage, cartilage degeneration, or prior surgery was excluded. Specimens were preserved at −20°C and thawed at room temperature 24 hours before testing. All soft tissue was removed from the specimens beyond 10 cm on either side of the joint line. The skin was removed from the knee joint, and the specimens were kept moist with 0.9% saline throughout testing. The tibial and femoral shafts were secured in bonding cement (Bondo; 3M), and the fixation was augmented with two 3.5-mm screws drilled transversely across each shaft. The fibula was stabilized with a 3.5-mm screw across the proximal syndesmosis, just above the cement fixation. Before testing, all knees underwent axial computed tomography (CT) scanning (Biograph; Siemens). Slice thickness was 0.625 mm.

The knees were mounted to a 6 degrees of freedom (DOF) robot (ZX165U; Kawasaki Robotics) equipped with a universal force-moment sensor (UFS) (Theta; ATI). The femur was rigidly fixed and the tibia was attached to the robotic arm. Robotic testing protocols, including coordinate system definitions, have been described previously.[15]

The passive flexion path of the intact knee was first defined from full extension to 90° of flexion by moving the tibia in 1°-flexion increments relative to the fixed femur. All knees were tested with clinically relevant loading conditions to simulate commonly performed stability examinations. Therefore, the Lachman and anterior drawer tests were simulated by applying a 134-N anterior load at 30° and 90° of flexion, respectively. Multiplanar valgus (8 N·m) and internal rotation (4 N·m) torques were applied at 15° of flexion to capture key aspects of the loads applied during the pivot-shift test.[19,27] This 2-torque model of the pivot shift causes anterior subluxation of the tibia,[7,17,25]

*Address correspondence to Danyal H. Nawabi, MD, FRCS, Sports Medicine and Shoulder Service, Department of Orthopaedic Surgery, Hospital for Special Surgery, 535 East 70th Street, New York, NY 10021, USA (email: nawabid@hss.edu).

†Department of Biomechanics, Hospital for Special Surgery, New York, New York, USA.

‡Sports Medicine and Shoulder Service, Department of Orthopaedic Surgery, Hospital for Special Surgery, Weill Medical College of Cornell University, New York, New York, USA.

a critical feature of the clinical pivot shift.[4] We alternated the order of kinematic testing from knee to knee.

The 5-DOF kinematics in response to these loading conditions applied to the ACL-intact knee were recorded. Subsequently, the medial femoral condyle was removed using a surgical oscillating saw to visualize the femoral insertion of the ACL. Membranous tissue covering the ACL was also removed at this stage.[24,34] All subsequent testing was performed with the robot operating in position control, and thus the position and orientation of the intact knee joint were the independent variables while loads measured across the joint were the dependent, measured variables. Since kinematics of the ACL-intact knee were determined before removing the medial femoral condyle, the robot could be instructed to repeat the motion path of the ACL-intact knee even after removing this portion of the bony anatomy.

A previous description of the relationship between the histologic and macroscopic anatomy of the ACL[31] was used to define our sectioning protocol referencing the location within the femoral footprint of the ACL (high or low). This was chosen because femoral tunnel location during ACL reconstruction is based on geographic location on the medial wall of the lateral femoral condyle. Sasaki et al[31] reported that the direct insertion bordered the lateral intercondylar ridge and measured an average of 5.3 mm in an anteroposterior direction. The indirect insertion commenced immediately posterior to the direct insertion and measured an average of 4.4 mm from the posterior aspect of the direct insertion to the posterior femoral articular cartilage margin. We therefore divided the femoral ACL footprint between the lateral intercondylar ridge and the posterior articular cartilage in half along a line perpendicular to the intercondylar ridge and defined an anterior band in the region of the direct fibers and a posterior extension in the region of the indirect fibers (Figure 1). The anterior band included a rectangular-shaped portion located higher within the ACL footprint paralleling the lateral intercondylar ridge and the remaining crescent-shaped tissue lower within the femoral footprint of the ACL extending along the posterior femoral cartilage. To divide the femoral footprint into higher and lower regions, the lateral intercondylar ridge and posterior articular margin were first identified. By drawing a tangent to the posterior aspect of the femoral condyle, parallel to the posterior femoral cortex at the roof of the notch, the maximum perpendicular distance between the ridge and tangent was measured using digital calipers (Fowler, Inc; accuracy = 20 μm, resolution = 10 μm, and repeatability = 10 μm). The midpoint of this line was used to delineate the high and low regions of the femoral footprint of the ACL. Although this assumption slightly overestimates the width of the indirect insertion according to the measurements of Sasaki et al,[31] it ensured that the direct fibers adjacent to the lateral intercondylar ridge would be included in the force measurements for the high region of the femoral footprint. All measurements were performed by a single observer (D.H.N.). All measurements were repeated 3 times with the measurer blinded to the individual values and then averaged.

After the high and low regions of the ACL footprint were identified, one of these regions was first sectioned using a No. 15 scalpel. The region that was sectioned first was
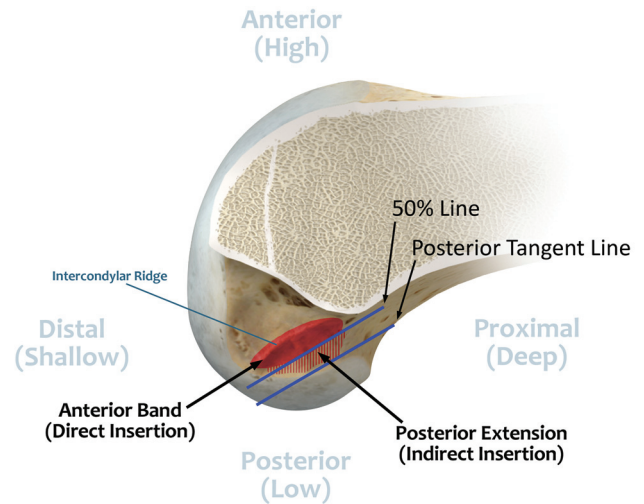

Figure 1. A schematic diagram of the lateral wall of the intercondylar notch is shown after removal of the medial femoral condyle. Orientation of the femur is indicated with the knee in 90° of flexion. The anterior band and posterior extension of the femoral insertion of the ACL are shown along with their relationship to the intercondylar ridge. The sectioning protocol identified the higher and lower fibers in the respective regions of the direct and indirect insertions of the ACL. This macroscopic division of the femoral footprint was achieved by dividing the perpendicular distance from the lateral intercondylar ridge to the posterior articular cartilage identified via a tangent to the posterior articular cartilage (posterior tangent line) in half (50% line).

alternated from specimen to specimen. The fibers within the low region (ie, low fibers) were sectioned with the knee extended by gradually dissecting back the crescent-shaped tissue from the posterior femoral cartilage to the previously marked 50% line (Figure 2, A and B). The fibers within the high regions (ie, high fibers) were sectioned by flexing the knee to 120° and gradually dissecting tissue from the femoral footprint until the 50% line was reached (Figure 2, C and D). The 5-DOF kinematics of the intact knee were repeated and loads across the knee measured for the simulated clinical examinations before and immediately after the high and low portions of the femoral insertion were sectioned. The order that the stability examinations of the intact knee were repeated was alternated from knee to knee. The vector difference of the force measured by the UFS before and after sectioning each portion of the ACL from its femoral insertion represents the force carried by the sectioned fibers[10]; however, this does not account for physical interaction between fibers.[6,29,30] Physical interaction of ACL fibers was accounted for by alternating sectioning order from specimen to specimen, as others have done.[15,35] If physical interaction exists, the drop in force caused by sectioning the high or low regions of the footprint of the femoral insertion would depend on section order.

The magnitude of the drop in force due to sectioning the fibers residing in the high and low regions of the femoral footprint was calculated. Moreover, since a primary function
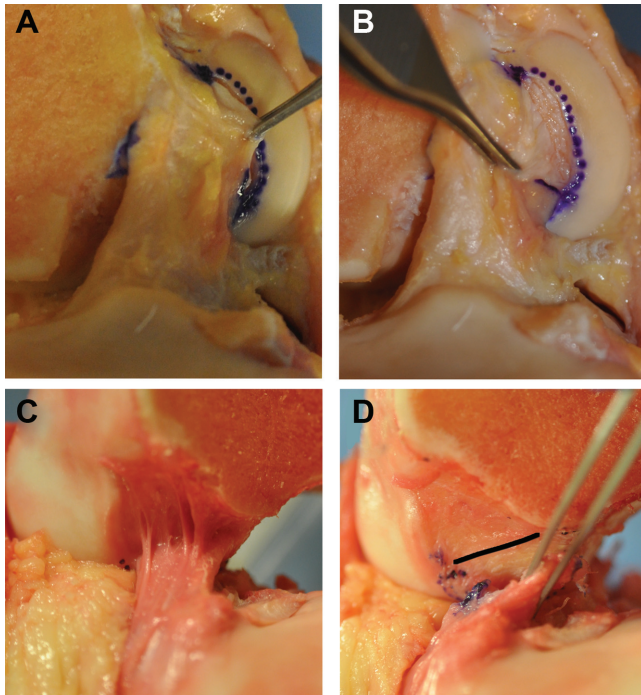
Figure 2. The crescent-shaped, low fibers of the femoral footprint of the ACL in the region of the indirect insertion (A) held in place with forceps and (B) subsequently flipped over, exposing the underlying bone. The high portion of the femoral footprint in the region of the direct fibers (C) before and (D) after sectioning. Image (C) shows membranous fibers that were removed to identify the lateral intercondylar ridge. The black line in image (D) identifies the lateral intercondylar ridge.

of the ACL is to restrain anterior translations of the tibia, the anteroposterior (AP) component of force carried by the high and the low fibers was determined. The AP component of force carried by the high and low regions of the ACL footprint was also reported as a percentage of the anterior load carried by the entire ACL. The forces carried by the high and low regions were also reported as a function of sectioning order to assess the presence of physical interaction between ACL fibers inserting into these regions.

Footprint Digitization and Validation of Sectioning Method

The borders of the sectioned areas were digitized using a 3-dimensional digitizer (MicroScribe G2X; Immersion) with accuracy of 0.23 mm after sectioning was completed and mapped onto a CT scan of each knee (Figure 3). Mapping of the digitized insertion onto the CT scan was performed via a fiducial marker rigidly fixed to the femur. The maximum positional error and rotational error of this method (mean ± SD) was −0.3 ± 1.4 mm and −0.1° ± 2.2°, respectively. The length of the lateral intercondylar ridge, the maximum perpendicular anteroposterior distance from the lateral intercondylar ridge to the posterior articular cartilage,
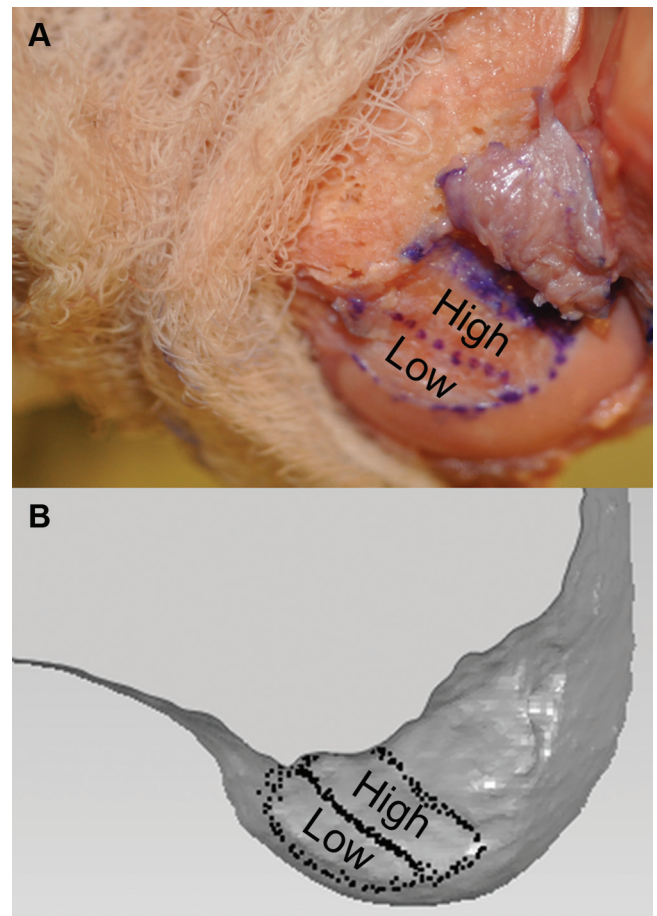

Figure 3. (A) A representative specimen with the high and low regions of the femoral footprint marked with ink identifying the geographic locations of the sectioned regions of the ACL footprint. The rectangular-shaped high portion of the footprint and the crescent-shaped lower portion of the footprint are shown. (B) Corresponding 3-dimensional computed tomography scan of the representative specimen overlaid with the manually digitized regions that were sectioned confirms the locations from which the high and low fibers were sectioned.

and the area of the femoral ACL footprint were calculated from the digitized CT scans (Geomagic Studio; Geomagic, Inc). The sectioning method was independently evaluated by 2 experienced observers (A.D.P. and T.L.W.), who confirmed that the digitized borders of the sectioned regions adhered to the sectioning method defined above. Each observer performed this evaluation while blinded to the results of the study to mitigate bias.

Isometry of Virtual ACL Fibers

Three-dimensional (3D) geometries of the femur and tibia were generated from the CT scan of each intact cadaveric knee (Mimics; Materialise, Inc). The 3D geometries were linked to their position and orientation along the passive
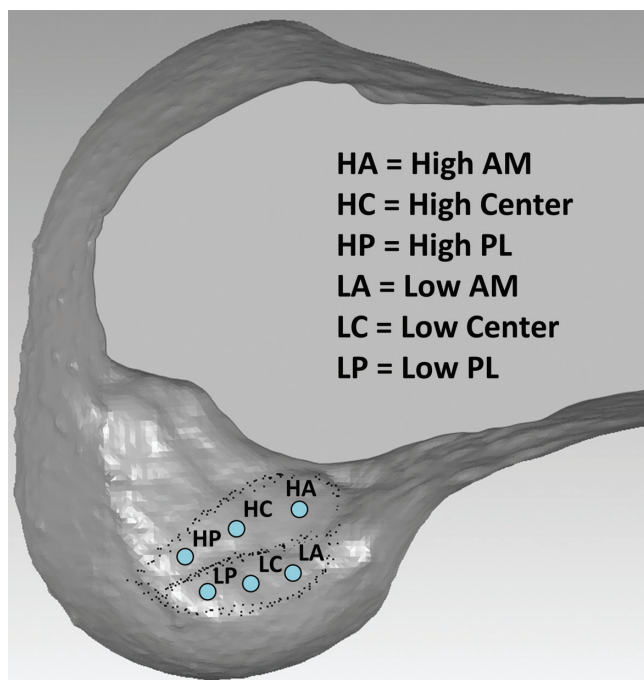
Figure 4. The 3 fiber locations each in the high and low regions of the femoral ACL footprint corresponding to the location of the direct and indirect insertions, respectively. The higher and lower regions of the femoral footprint of the ACL were divided in thirds along their length and the center of each of these sections was identified as the fiber attachment points. AM, anteromedial; PL, posterolateral.

flexion path during robotic testing via the fiducial markers described above. Three femoral attachment points were selected in the high and low regions of the femoral footprint of the ACL (Figure 4). We subdivided both the high and low regions into thirds from proximal to distal and took the center of each of these subsections as the fiber attachment points on the femur. Virtual fibers were placed between each femoral attachment point and a tibial point corresponding to a central tibial tunnel position. The length of each virtual fiber was calculated at 0°, 15°, 30°, and 90° of flexion. Subsequently, the difference between the maximum and minimum length of each virtual fiber across these 4 flexion angles was determined for each attachment point as previously reported.[14] This yielded a maximum change in length for each virtual fiber location. The maximum change in length was also normalized relative to the virtual fiber length at full extension as this flexion angle is commonly used for graft fixation in ACL reconstruction surgery.

Statistical Methods

Forces carried by the high and low regions of the femoral ACL footprint and maximum changes in virtual fiber length were expressed as means ± standard deviations. For each simulated clinical examination, forces were compared between high and low regions using paired t tests.
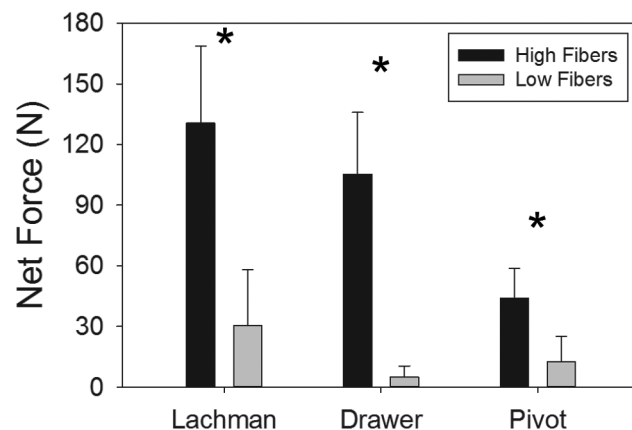

Figure 5. Mean resultant load transferred across the high and low portion of the femoral ACL insertion (high fibers and low fibers, respectively) when applying an anterior load at 30° and 90° of flexion (Lachman and anterior drawer tests, respectively) and a combined valgus and internal rotation moment at 15° of flexion (pivot-shift test). *Statistically significant difference ($P < .05$). Whiskers indicate 1 SD.

Forces carried by the high and low regions were compared as a function of sectioning order using unpaired t tests. The maximum changes in length of the virtual graft fibers across each of the 6 fiber locations within the femoral footprint were compared using a 1-way analysis of variance model with Tukey post hoc adjustment. Statistical significance was set to $\alpha \le .05$ for all comparisons.

RESULTS

The net force carried by the ACL in response to an applied anterior force at 30° of flexion (simulated Lachman test) averaged 159.5 ± 30.4 N with the high fibers carrying 100.1 ± 58.9 N more net force than the low fibers ($P < .001$) (Figure 5). The high fibers carried 81.3% ± 17.0% of the anterior force carried by the ACL (Figure 6), which corresponded to 81.7 ± 46.5 N more anterior force carried by the high fibers than the low fibers ($P < .001$) during this simulated Lachman test. When the high fibers were sectioned first, the high fibers carried 66.3% ± 9.5% of the anterior force carried by the ACL ($P = .019$) (Table 1). When the low fibers were sectioned first, the high fibers carried 96.2% ± 0.7% of the anterior force carried by the ACL ($P < .001$).

The net force carried by the ACL in response to an applied anterior force at 90° of flexion (simulated anterior drawer test) averaged 109.0 ± 28.9 N with the high fibers carrying 100.4 ± 10.4 N more net force than the low fibers ($P < .001$) (Figure 5). The high fibers carried 96.0% ± 6.0% of the anterior component of force carried by the ACL (Figure 6), which corresponded to 95.0 ± 31.6 N more anterior force carried by the high fibers than the low fibers ($P < .001$) during this simulated anterior drawer test. When the high fibers were sectioned first, the high fibers carried

TABLE 1
Anterior Component of Force Carried by High and Low Fibers Based on Sectioning Order[a]

	High Fibers Sectioned First (n = 5)			Low Fibers Sectioned First (n = 5)		
	High Fibers, N	Low Fibers, N	P Value	High Fibers, N	Low Fibers, N	P Value
Lachman test	88.4 ± 19.6 (71.2 to 105.6)	46.1 ± 20.7 (28.0 to 64.2)	.019	126.0 ± 20.3 (108.2 to 143.8)	5.0 ± 1.3 (3.9 to 6.1)	<.001
Anterior drawer test	116.3 ± 18.9 (99.7 to 132.9)	2.0 ± 2.8 (−0.5 to 4.5)	<.001	80.7 ± 28.0 (56.2 to 105.2)	5.0 ± 6.9 (−1.0 to 11.0)	.005
Pivot-shift test	33.1 ± 15.8 (19.3 to 46.9)	13.8 ± 11.6 (3.6 to 24.0)	.041	27.8 ± 5.0 (23.4 to 32.2)	2.9 ± 1.7 (1.4 to 4.4)	<.001

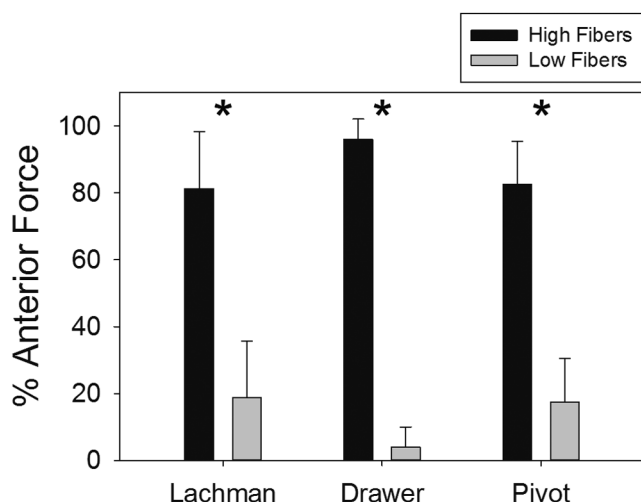[a]Data are reported as mean ± SD (95% CI).

Figure 6. Mean percentage of anterior load transferred across the high and low portion of the femoral ACL insertion (high fibers and low fibers, respectively) relative to the total anterior load carried by the ACL. Percentages are determined in response to an applied anterior load at 30° and 90° of flexion (Lachman and anterior drawer tests, respectively) and a combined valgus and internal rotation moment at 15° of flexion (pivot-shift test). *Statistically significant difference ($P < .05$). Whiskers indicate 1 SD.

98.1% ± 2.8% of the anterior force carried by the ACL ($P = .001$) (Table 1). When the low fibers were sectioned first, the high fibers carried 94.0% ± 8.0% of the anterior force carried by the ACL ($P = .005$).

The net force carried by the ACL in response to combined valgus and internal rotation torques at 15° of flexion was 55.0 ± 19.8 N with the high fibers carrying 31.2 ± 19.0 N more force than the low fibers ($P = .001$) (Figure 5). The high fibers carried 82.5% ± 12.9% of the anterior component of force carried by the ACL (Figure 6), which corresponded to 22.1 ± 10.5 N more anterior force carried by the high fibers than the low fibers ($P < .001$) during this simulated pivot shift (Figure 5). When the high fibers were sectioned first, the high fibers carried 74.0% ± 13.3% of the anterior force carried by the ACL ($P = .041$) (Table 1).

When the low fibers were sectioned first, the high fibers carried 91.0% ± 4.3% of the anterior force carried by the ACL ($P = .001$).

Isometry of Virtual ACL Fibers

Virtual ACL fibers placed at the high AM location of the femoral footprint were the most isometric, having a mean maximum change in length of 3.9 ± 1.5 mm (Figure 7) with a normalized value of 10.9% ± 4.6%. The high AM location was more isometric than all 3 locations in the low region of the femoral footprint ($P < .001$). The mean maximum length change of virtual fibers placed at the high center location was 5.4 ± 1.7 mm with a normalized value of 16.3% ± 5.9%. The high center location was more isometric than the mean maximum change in length at the low posterolateral (PL) and low center locations (both $P < .001$). The maximum change in length of virtual fibers placed in the high PL location averaged 7.3 ± 1.9 mm with a normalized value of 23.7% ± 7.3%. This was 3.4 mm less isometric than the high AM position ($P < .001$).

Digitization Measurements

The length of the lateral intercondylar ridge ranged from 17.1 to 27.0 mm (Table 2). The maximum distance from the lateral intercondylar ridge to the posterior femoral articular cartilage ranged from 10.0 to 14.8 mm. The area of the femoral ACL footprint ranged from 161.8 to 293.8 mm².

DISCUSSION

This study has shown that the high fibers of the femoral footprint of the ACL (anterior band) neighboring the lateral intercondylar ridge carry more force than the low, crescent-shaped fibers (posterior extension) in response to simulated Lachman, anterior drawer, and pivot-shift tests. Furthermore, virtual ACL fibers located in the high AM portion of the femoral footprint of the ACL are more isometric than fibers placed in the lower region of the femoral footprint. Although additional biomechanical and clinical data are needed, these results suggest that higher
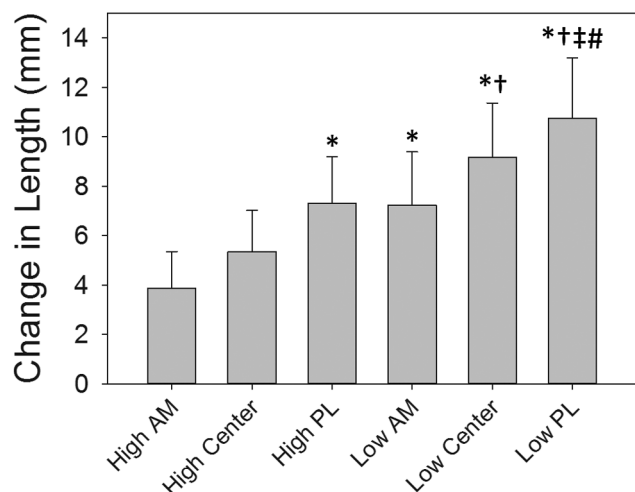
Figure 7. Mean maximum elongation of virtual ACL fibers located at the 3 high and the 3 low tunnel locations. Statistically significant difference ($P < .05$) compared with *high anteromedial (AM), †high center, ‡high posterolateral (PL), and #low AM. Whiskers indicate 1 SD. Two fiber locations with differences in maximum elongation that were more than twice the uncertainty in our registration method (±1.4 mm) were considered different.

TABLE 2
Native ACL Femoral Footprint Dimensions
for All 10 Cadaveric Specimens

Specimen	Ridge Length, mm	Ridge to Cartilage, mm	Area of Footprint, mm^2
1	22.6	13.9	255.9
2	27.0	14.8	293.8
3	17.1	13.0	218.4
4	23.9	10.0	196.6
5	18.7	12.3	182.5
6	19.7	11.4	206.2
7	18.9	14.3	161.8
8	24.5	12.1	254.5
9	23.5	13.7	244.2
10	23.7	12.6	246.8
Mean ± SD	21.9 ± 3.2	12.9 ± 2.0	226.1 ± 40.0

graft placement in the region of the high fibers of the femoral insertion of the ACL could provide the best compromise between reconstructing that portion of the ACL that bears the most load during stability examinations, yet remains the most isometric through passive knee flexion.

Similar to Kawaguchi et al,[18] when we sectioned the low fibers from the ACL footprint first, these low fibers provided little resistance to applied anterior tibial translations at 30° and 90° of flexion, while the high fibers contributed most of the resisting force (Figure 7). Interestingly, at 30° of flexion, when we switched sectioning order and sectioned the high fibers first, these high fibers still carried the majority of force; however, the low fibers carried additional force (Table 1). The dependency of load carried by the high and low fibers on section order may suggest physical interaction across the ACL midsubstance. This observation merits further investigation with more refined methods for identifying and sectioning specific ACL fibers. Pathare et al[27] reported limited changes in anterior and rotational kinematics after isolated sectioning of the low fibers in the region of the indirect insertion. This supports our finding that the high fibers play a dominant role in resisting loads applied during simulated clinical examinations.

The isometry analysis performed in this study showed that the high AM tunnel position was the most isometric during passive range of motion and is more isometric than all 3 lower tunnel positions within the region of the indirect insertion (Figure 7). This finding corroborates studies that have shown large changes in the length of ACL grafts placed anatomically.[21,37] The classic study by Artmann and Wirth[3] showed that the interinsertional distance between the center of the tibial footprint of the ACL

and "lower" femoral locations can decrease by about 9 mm as the knee flexes from 0° to 120°. The findings also agree with previous work that identified the high AM region to be the most isometric through passive flexion with greater anisometry near the posterior femoral cartilage in the low center region defined in this study.[14,32,39] Markolf et al[22] also showed that a single AM-bundle ACL reconstruction experienced forces and changes in length that were closest to the native ACL and lower than an anatomic double-bundle reconstruction, in which the PL-bundle graft occasionally failed in tests near zero degrees. Thus, "low" ACL grafts in the region of the indirect femoral ACL insertion may experience greater forces due to greater length changes.[2]

Altogether, our data and the previous literature summarized above indicate that the high fibers of the femoral footprint of the ACL neighboring the lateral intercondylar ridge (1) take up the majority of force during the Lachman and pivot examination, (2) play a dominant role in controlling translations and rotations during the Lachman and pivot examination, and (3) represent the most isometric region of the footprint.

Our results may support avoiding low graft placement since this region of the femoral footprint bears less force during stability examinations and is more anisometric than the high region of the femoral footprint. Indeed, the trend toward "lower" femoral tunnels may prove detrimental to the graft as recent biomechanical studies have shown significantly greater length changes and resultant force in anatomic (ie, lower) grafts during range of motion.[21,22,37] Of greater concern has been the report from the Danish Knee Ligament Reconstruction Registry that showed that the cumulative revision rate for AM portal ACL reconstruction, which may be associated with "lower" placement of femoral tunnels,[5] has led to increased rates of graft failure after 4 years of 5.16% compared with 3.20% for transtibial techniques in a total of 9239 ACL reconstructions.[28]

This study has limitations. We relied on previously published measures of the regional location of the direct and indirect insertion fibers as our guide to detach portions of the ACL from the femoral footprint.[31] Thus, there may

have been error in isolating those regions where only direct and only indirect fibers reside. However, using geographic locations of the femoral footprint instead of the fiber type is potentially more clinically applicable since tunnel location during ACL reconstruction is based on macroscopic visualization of the medial wall of the lateral femoral condyle. Moreover, ACL rupture disturbs the ligament fibers, which would make it more difficult to distinguish any specific fiber type.

Sectioning the ACL solely from the femoral footprint allows for potential physical interaction between fibers within the ACL substance. We accounted for physical interaction by defining a sectioning method that was corroborated via CT and direct footprint digitization and by alternating the order of sectioning. This approach has also been taken by others to assess the level of physical interaction.[11,30] Overall, our sectioning method allowed us to avoid identifying and isolating fibers coursing through the ACL substance and into the direct and indirect femoral insertions, which would likely have been difficult given the complexity of the fibers composing the ACL.[1,12] However, failure to section all of the direct fibers when detaching the high portion of the ACL footprint could contribute to the difference between loading across the high and low regions of the femoral footprint as a function of sectioning order. This could specifically account for the decreased load in the high fibers in the region of the direct insertion when this tissue was sectioned first compared with when it was sectioned second (Table 1). Overall, our approach closely matched but conservatively estimated the size of the indirect insertion based on the measurements of Sasaki et al.[31] Even with this conservative assessment, which would be susceptible to leaving direct fibers in the low portion of the anatomic footprint of the femoral insertion of the ACL when sectioning the high region of the ACL footprint, the majority of load was still carried by the tissue located in the high region of the anatomic footprint and does not alter the main conclusion of this study. More accurate means of identifying specific fibers residing within the femoral footprint would help to better isolate the source of the section-order dependency of load across the fibers residing in the high and low regions of the femoral footprint. Robot and bone stiffness, as well as accuracy of the algorithms used to control the robot, may affect force measurements; however, our repeatability assessment of ACL force in response to 5 repetitions of the combined valgus and internal rotation torques was ±4.1 N. This is 4.7 times below the smallest differences in load between the high and low regions of the femoral footprint (Table 1). Moreover, the path of passive flexion defined with our robotic testing protocol agreed with previous work reporting coupled internal tibial rotation with flexion primarily from full extension to about 30° of flexion[35]; therefore, these data represent a typical passive flexion path. The resultant ACL force was higher than the applied anterior force; however, this has been reported in previous studies and likely occurs because the ACL is not parallel to the applied anterior load.[10,20,30] Wrapping is not accounted for in our assessment of isometry; therefore, our measurements are a lower estimate of the level of anisometry. Even in this conservative scenario, there are differences in isometry for the insertion points; thus, these data still help to elucidate how grafts located in these regions may function. Differences in isometry between the high AM insertion point and any low insertion (AM, center, and PL) were 3.4 to 6.9 mm. Thus, the differences in anisometry between these locations were at least 2.4 times more than the uncertainty in the registration process (±1.4 mm) and would not affect our conclusions.

Our speculation on appropriate femoral tunnel location can only be confirmed by evaluating the biomechanical characteristics of actual grafts placed at the locations suggested in this study, followed by controlled clinical studies. Finally, additional biomechanical testing at a wider range of flexion angles in response to more complex, loading conditions such as pivoting maneuvers that include rotations coupled with flexion[27] must be performed to further elucidate load transfer characteristics at these insertion sites and the relevance of any potential intrasubstance fiber interaction.

In conclusion, high ACL fibers within the femoral footprint carry more force during stability testing than fibers in the low region of the femoral footprint. Virtual fibers placed in the high AM location are more isometric than in the low location during range of motion. These findings may suggest that placing a graft in the region of the direct insertion, encroaching on the lateral intercondylar ridge but clear of the posterior articular margin, may achieve a compromise between reconstructing that portion of the ACL that bears the most force during stability examinations, yet remains the most isometric through passive flexion.

REFERENCES

1. Appel M, Gradinger R. Architektur des Kreuzbandaufbaus. *Prakt Sport Traum Sportmed*. 1989;1:19-23.
2. Araujo PH, Asai S, Pinto M, et al. ACL graft position affects in situ graft force following ACL reconstruction. *J Bone Joint Surg Am*. 2015;97(21):1767-1773.
3. Artmann M, Wirth CJ. Investigation of the appropriate functional replacement of the anterior cruciate ligament [author's transl]. *Z Orthop Ihre Grenzgeb*. 1974;112(1):160-165.
4. Bedi A, Musahl V, Lane C, Citak M, Warren RF, Pearle AD. Lateral compartment translation predicts the grade of pivot shift: a cadaveric and clinical analysis. *Knee Surg Sports Traumatol Arthrosc*. 2010;18(9):1269-1276.
5. Bowers AL, Bedi A, Lipman JD, et al. Comparison of anterior cruciate ligament tunnel position and graft obliquity with transtibial and anteromedial portal femoral tunnel reaming techniques using high-resolution magnetic resonance imaging. *Arthroscopy*. 2011;27(11):1511-1522.
6. Debski RE, Sakone M, Woo SL, Wong EK, Fu FH, Warner JJ. Contribution of the passive properties of the rotator cuff to glenohumeral stability during anterior-posterior loading. *J Shoulder Elbow Surg*. 1999;8(4):324-329.
7. Engebretsen L, Wijdicks CA, Anderson CJ, Westerhaus B, LaPrade RF. Evaluation of a simulated pivot shift test: a biomechanical study. *Knee Surg Sports Traumatol Arthrosc*. 2012;20(4):698-702.
8. Farrow LD, Chen MR, Cooperman DR, Victoroff BN, Goodfellow DB. Morphology of the femoral intercondylar notch. *J Bone Joint Surg Am*. 2007;89(10):2150-2155.
9. Fu FH, Jordan SS. The lateral intercondylar ridge—a key to anatomic anterior cruciate ligament reconstruction. *J Bone Joint Surg Am*. 2007;89(10):2103-2104.

10. Fujie H, Livesay GA, Woo SL, Kashiwaguchi S, Blomstrom G. The use of a universal force-moment sensor to determine in-situ forces in ligaments: a new methodology. *J Biomech Eng*. 1995;117(1):1-7.

11. Gabriel MT, Wong EK, Woo SL, Yagi M, Debski RE. Distribution of in situ forces in the anterior cruciate ligament in response to rotatory loads. *J Orthop Res*. 2004;22(1):85-89.

12. Hara K, Mochizuki T, Sekiya I, Yamaguchi K, Akita K, Muneta T. Anatomy of normal human anterior cruciate ligament attachments evaluated by divided small bundles. *Am J Sports Med*. 2009;37(12):2386-2391.

13. Harner CD, Baek GH, Vogrin TM, Carlin GJ, Kashiwaguchi S, Woo SL. Quantitative analysis of human cruciate ligament insertions. *Arthroscopy*. 1999;15(7):741-749.

14. Hefzy MS, Grood ES. Sensitivity of insertion locations on length patterns of anterior cruciate ligament fibers. *J Biomech Eng*. 1986; 108(1):73-82.

15. Imhauser C, Mauro C, Choi D, et al. Abnormal tibiofemoral contact stress and its association with altered kinematics after center-center anterior cruciate ligament reconstruction: an in vitro study. *Am J Sports Med*. 2013;41(4):815-825.

16. Iwahashi T, Shino K, Nakata K, et al. Direct anterior cruciate ligament insertion to the femur assessed by histology and 3-dimensional volume-rendered computed tomography. *Arthroscopy*. 2010;26(9) (suppl):S13-S20.

17. Kanamori A, Woo SL, Ma CB, et al. The forces in the anterior cruciate ligament and knee kinematics during a simulated pivot shift test: a human cadaveric study using robotic technology. *Arthroscopy*. 2000;16(6):633-639.

18. Kawaguchi Y, Kondo E, Takeda R, Akita K, Yasuda K, Amis AA. The role of fibers in the femoral attachment of the anterior cruciate ligament in resisting tibial displacement. *Arthroscopy*. 2015;31(3):435-444.

19. Lane CG, Warren R, Pearle AD. The pivot shift. *J Am Acad Orthop Surg*. 2008;16(12):679-688.

20. Livesay GA, Fujie H, Kashiwaguchi S, Morrow DA, Fu FH, Woo SL. Determination of the in situ forces and force distribution within the human anterior cruciate ligament. *Ann Biomed Eng*. 1995;23(4):467-474.

21. Lubowitz JH. Anatomic ACL reconstruction produces greater graft length change during knee range-of-motion than transtibial technique. *Knee Surg Sports Traumatol Arthrosc*. 2014;22(5):1190-1195.

22. Markolf KL, Park S, Jackson SR, McAllister DR. Anterior-posterior and rotatory stability of single and double-bundle anterior cruciate ligament reconstructions. *J Bone Joint Surg Am*. 2009;91(1):107-118.

23. Mochizuki T, Fujishiro H, Nimura A, et al. Anatomic and histologic analysis of the mid-substance and fan-like extension fibres of the anterior cruciate ligament during knee motion, with special reference to the femoral attachment. *Knee Surg Sports Traumatol Arthrosc*. 2014;22(2):336-344.

24. Mochizuki T, Muneta T, Nagase T, Shirasawa S, Akita KI, Sekiya I. Cadaveric knee observation study for describing anatomic femoral tunnel placement for two-bundle anterior cruciate ligament reconstruction. *Arthroscopy*. 2006;22(4):356-361.

25. Noyes FR, Jetter AW, Grood ES, Harms SP, Gardner EJ, Levy MS. Anterior cruciate ligament function in providing rotational stability

assessed by medial and lateral tibiofemoral compartment translations and subluxations. *Am J Sports Med*. 2015;43(3):683-692.

26. Odensten M, Gillquist J. Functional anatomy of the anterior cruciate ligament and a rationale for reconstruction. *J Bone Joint Surg Am*. 1985;67(2):257-262.

27. Pathare NP, Nicholas SJ, Colbrunn R, McHugh MP. Kinematic analysis of the indirect femoral insertion of the anterior cruciate ligament: implications for anatomic femoral tunnel placement. *Arthroscopy*. 2014;30(11):1430-1438.

28. Rahr-Wagner L, Thillemann TM, Pedersen AB, Lind MC. Increased risk of revision after anteromedial compared with transtibial drilling of the femoral tunnel during primary anterior cruciate ligament reconstruction: results from the Danish Knee Ligament Reconstruction Register. *Arthroscopy*. 2013;29(1):98-105.

29. Rudy TW, Livesay GA, Woo SL, Fu FH. A combined robotic/universal force sensor approach to determine in situ forces of knee ligaments. *J Biomech*. 1996;29(10):1357-1360.

30. Sakane M, Fox RJ, Woo SL, Livesay GA, Li G, Fu FH. In situ forces in the anterior cruciate ligament and its bundles in response to anterior tibial loads. *J Orthop Res*. 1997;15(2):285-293.

31. Sasaki N, Ishibashi Y, Tsuda E, et al. The femoral insertion of the anterior cruciate ligament: discrepancy between macroscopic and histological observations. *Arthroscopy*. 2012;28(8):1135-1146.

32. Sidles JA, Larson RV, Garbini JL, Downey DJ, Matsen FA III. Ligament length relationships in the moving knee. *J Orthop Res*. 1988; 6(4):593-610.

33. Siebold R, Ellert T, Metz S, Metz J. Femoral insertions of the anteromedial and posterolateral bundles of the anterior cruciate ligament: morphometry and arthroscopic orientation models for double-bundle bone tunnel placement—a cadaver study. *Arthroscopy*. 2008;24(5):585-592.

34. Smigielski R, Zdanowicz U, Drwiega M, Ciszek B, Ciszkowska-Lyson B, Siebold R. Ribbon like appearance of the midsubstance fibres of the anterior cruciate ligament close to its femoral insertion site: a cadaveric study including 111 knees. *Knee Surg Sports Traumatol Arthrosc*. 2015;23(11):3143-3150.

35. Wilson DR, Feikes JD, Zavatsky AB, O'Connor JJ. The components of passive knee movement are coupled to flexion angle. *J Biomech*. 2000;33(4):465-473.

36. Woo SL, Gomez MA, Sites TJ, Newton PO, Orlando CA, Akeson WH. The biomechanical and morphological changes in the medial collateral ligament of the rabbit after immobilization and remobilization. *J Bone Joint Surg Am*. 1987;69(8):1200-1211.

37. Xu Y, Liu J, Kramer S, et al. Comparison of in situ forces and knee kinematics in anteromedial and high anteromedial bundle augmentation for partially ruptured anterior cruciate ligament. *Am J Sports Med*. 2011;39(2):272-278.

38. Yasuda K, Kondo E, Ichiyama H, et al. Anatomic reconstruction of the anteromedial and posterolateral bundles of the anterior cruciate ligament using hamstring tendon grafts. *Arthroscopy*. 2004;20(10):1015-1025.

39. Zavras TD, Race A, Bull AM, Amis AA. A comparative study of 'isometric' points for anterior cruciate ligament graft attachment. *Knee Surg Sports Traumatol Arthrosc*. 2001;9(1):28-33.